SEMI-ANALYTIC SOLUTION OF NON-REGULARIZED UNFOLDING STRESSES IN COMPOSITE BEAMS EMPLOYING A SERIES APPROXIMATION BASED ON LEGENDRE POLYNOMIALS

Juan M. González-Cantero[1, 2], Enrique Graciani[2], Federico París[2], Bernardo López-Romano[1] and Daniel Meizoso-Latova[3]

[1]FIDAMC, Tecnogetafe, Avda. Rita Levi-Montalcini 29, 28906, Getafe, Madrid, Spain
Email: Juan.Manuel.Gonzalez@fidamc.es, web page: http://www.fidamc.es

[2]Grupo de Elasticidad y Resistencia de Materiales
Universidad de Sevilla, Camino de los Descubrimientos s/n, 41092 Sevilla, Spain

[3]Airbus, Paseo John Lennon s/n, 28906, Getafe, Madrid, Spain

Keywords: Composite beams, Curved beam, Edge effects, Semi-analytic solution, Unfolding failure

ABSTRACT

Unfolding is one of the main causes of failure on composite beams including curved parts in their sections, such as L-beams, T-beams or C-beams, it being in many cases the critical criterion in the sizing of this kind of beams. This failure mechanism is caused by the interlaminar normal and shear stresses. Regularized interlaminar stresses are predicted in a very accurate way with current methods, but typical edge effects make those regularized stresses inaccurate with errors even by 100%. An illustrative example is the joint of a straight and a curved beam, as in the section of L-beams, where the compatibility between the two beams modifies the stress distribution which become significantly different to the regularized stresses. This study presents the fundamentals and the results of a novel semi-analytic method that predicts in a very accurate way the non-regularized stresses in 2D composite laminates of constant thickness and treated as a sequence of several constant-curvature beams. This method is a powerful tool to predict the unfolding failure in composite beams containing curved parts in their sections, with the same or better accuracy than using finite elements.

1 INTRODUCTION

Composite materials are designed to bear high intralaminar loads, with a very good strength-weight ratio. However, composite laminates usually have, in comparison, very low strengths in the interlaminar direction. Typical laminate models do not consider interlaminar stresses (see [1], Chapter 4). Nevertheless, when the geometry of the laminate includes curved parts with a relatively small ratio between the radius, R, and the thickness, t, significant interlaminar stresses appear and can provoke a delamination called unfolding failure (see [2]).

For anisotropic lineal homogeneous materials, the stresses in a 2D curved beam were firstly predicted by Lekhnitskii (see [3], Chapter 3). Lekhnitskii's equations have been widely used in the calculation of the interlaminar stresses in composite laminates. However, composite laminates are not homogeneous, and the stacking sequence affects significantly the stress distribution, and, accordingly, the failure load. This effect cannot be predicted with Lekhnitskii's equations.

First models for evaluating interlaminar stresses in composite curved beams considered the hypothesis of thin laminates ($t \ll R$), obtaining intralaminar equations similar to those of the classical laminate theory (see [4]). However, typical curved laminates under unfolding failure have small R/t ratios, introducing errors about 5% due to this fact. More recent theories considered the effect of the curvature in interlaminar stresses (see [5]), obtaining logarithmic equations in the calculus of the stiffnesses needed for determining the intralaminar stresses (see [6], Chapter 3.2.1). Using these stiffnesses, the coupling terms in the behaviour equations of the axial force and the bending moments do not vanish when a symmetrical laminate is chosen, effect that becomes higher when the R/t ratio decreases. These theories have errors over 5% for typical stacking sequences.

Finally, an exact model for the calculation of the interlaminar stresses in 2D composite curved laminates under axial and shear forces and bending moment was developed (see [7, 8]), based on an extension of the Lekhnitskii stress functions. These models calculate the solution of intralaminar and interlaminar stresses in an isolated and loaded curved laminate beam. However, the reality shows that in some cases the calculus of the unfolding failure with those methods may have errors even by 100%. These errors are due to the edge-effects appearing at the ends of the laminates or in zones with curvature changes that the models do not take into account. In other words, previous methods calculate regularized stresses, but the changes in the curvature introduce perturbations on the stress distribution, similar to an edge-effect. An illustrative case is the L-beam, where the section is composed of a curved beam joined to two straight beams. The joints, where a curvature change takes place, provoke the appearance of edge-effects and, therefore, of non-regularized stresses. Interlaminar stresses decrease in this zone, in a transition between the regularized interlaminar stresses in the curved beam and the null interlaminar stresses in the straight beams. These effects can be confirmed using Elements models, which (although not shown here for the sake of brevity) have been utilized to check the accuracy of the semi-analytical method developed.

The exact model for regularized stresses, previously mentioned, is extremely difficult to extend to the calculation of the non-regularized stresses due to the necessity of having the stress functions for these cases. In that way, a simpler model for the regularized stresses based on a curvature modification of the beam theory was developed by the authors in [9, 10], which is easier to extend to determine the non-regularized stresses. This extension (see [11]) is based on a series expansion of the displacements. Several authors have worked in that series expansion in a higher-order theory (see [12]). However, these theories are based on monomial functions in the series expansion. A study done in [11] shows that monomial functions induce high condition numbers in the stiffness matrices when the maximum order considered on the monomial functions increases, what results in the appearance of numerical instabilities. A solution to this problem is the modification of the series expansion by expressing it as a sum of Legendre polynomials.

The model developed in [11] defines higher-order moments of the 2D stress components to close the problem. The results obtained with this model are shown in this paper for three configurations in which the non-regularized stresses may become significantly different from the regularized stresses.

2 MODEL DEVELOPMENT

The problem to be solved consists on a curved 2D composite beam of constant thickness, t, under end axial, N_0, and shear, Q_0, forces and bending moment, M_0. The beam is composed by several beams of constant curvature, e.g., an L-shaped section is composed of two straight beams and one curved beam of constant curvature, or the section of a joggle is typically composed of three straight beams and two curved beams of constant curvature (see Figure 1), i.e., those beams are composed of a chain of beams of constant curvature. Normally, the first and the last beam of the chain are straight beams that can be considered as sufficiently long. Therefore, stresses tend to their regularized value far from the extremes connected to the curved parts of the beam.

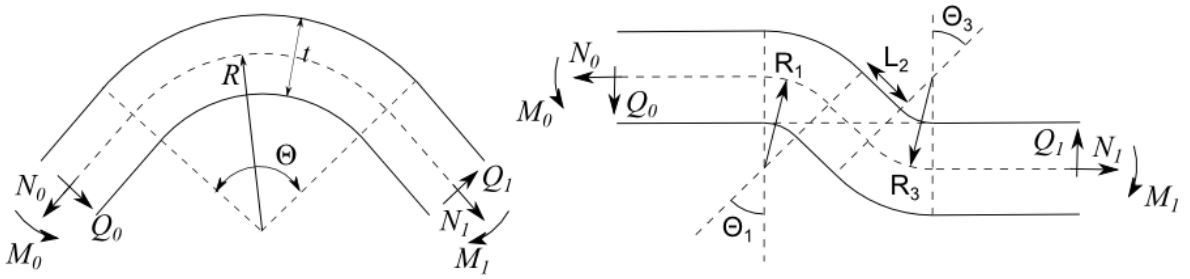

(a) (b)

Figure 1: Examples of problems considered in the model: (a) L-shaped section, (b) joggle.

The resolution is carried out supposing a generic boundary condition in circumferential and shear stresses in every beam of the chain, solving the equations in those beams, and equaling the stresses and displacements between every pair of adjacent beams to determine the real boundary conditions. Therefore, every beam is first solved individually, with generic boundary conditions, see Figure 2.

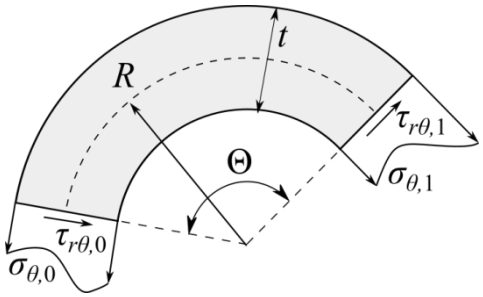

Figure 2: Generic boundary conditions in an individual and finite curved beam.

Typical beam models use the Euler–Bernoulli beam theory (see [13]) or the Timoshenko beam theory (see [14, 15]), where displacements are approached considering that the thickness remains constant and that cross sections remain straight:

$$u(\theta,z) = u_o(\theta) + zu_1(\theta) \quad , \quad w(\theta,z) = w_o(\theta) \, , \tag{1}$$

where $0 < \theta < \Theta$ and z is the through-thickness coordinate, defined in a curved beam from the radial coordinate as $z = r - R$. R is the medium radius, u is the circumferential displacement and w the radial displacement.

The strains calculated from the previous displacements in a curved beam are given by:

$$\varepsilon_\theta(\theta,z) = \frac{1}{r}\frac{\partial u}{\partial \theta} + \frac{w}{r} = \frac{R}{r}\left(\varepsilon_\theta^o(\theta) + z\varepsilon_\theta^1(\theta)\right) , \tag{2a}$$

$$\varepsilon_r(\theta,z) = \frac{\partial w}{\partial r} = 0 \, , \tag{2b}$$

$$\gamma_{r\theta}(\theta,z) = \frac{\partial u}{\partial r} - \frac{u}{r} + \frac{1}{r}\frac{\partial w}{\partial \theta} = \frac{R}{r}\gamma_{r\theta}^o(\theta). \tag{2c}$$

Notice that the circumferential strain ε_θ is approximated by two θ-dependent terms, the shear strain $\gamma_{r\theta}$ by only one and the radial strain ε_r is null.

The model developed in [11] considers the approximation of the circumferential displacements based on a series expansion of Legendre polynomials, $p_i(\hat{z})$ (see [16]). Legendre polynomials are defined in the range $-1 < \hat{z} < 1$. Therefore, the through-thickness coordinate z (and accordingly all lengths and displacements of the problem) have been adimensionalized with $t/2$. In that way, $\hat{z} = 2z/t$. In the following, the hat is employed to denote dimensionless magnitudes. Hence, circumferential displacements are given by:

$$\hat{u}(\theta,\hat{z}) = \hat{u}_o(\theta) + \hat{z}\hat{u}_1(\theta) + \textstyle\sum_{i=2}^{n} p_i(\hat{z})\hat{u}_i(\theta) \, , \tag{3}$$

where n is defined as the method order.

Notice that the Timoshenko beam theory is obtained when $n = 1$ and that the model converges to the exact solution when the model order increases. To get the same number of equations than unknown variables (taking into account the number of forces defined later) it is necessary that the circumferential strain is approached by $n+1$ θ-dependent terms, the radial strain by $n-1$ θ-dependent terms and the shear strain by n θ-dependent terms. These conditions are satisfied by using the next radial displacement approximation (see [11]):

$$\hat{w}(\theta,\hat{z}) = \hat{w}_o(\theta) + \textstyle\sum_{i=1}^{n-1} f_i(\hat{z})\hat{w}_i(\theta) \, , \tag{4a}$$

$$f_i(\hat{z}) = p_i(\hat{z}) + \frac{1}{(2i+1)\hat{R}}\left(ip_{i+1}(\hat{z}) + (i+1)p_{i-1}(\hat{z})\right) . \tag{4b}$$

Therefore, the circumferential, radial and shear strains can be obtained as:

$$\varepsilon_\theta(\theta,\hat{z}) = \frac{1}{\hat{r}}\frac{\partial \hat{u}}{\partial \theta} + \frac{\hat{w}}{\hat{r}} = \frac{\hat{R}}{\hat{r}}\left(\varepsilon_\theta^o(\theta) + \hat{z}\varepsilon_\theta^1(\theta) + \sum_{i=2}^{n} p_i(\hat{z})\varepsilon_\theta^i(\theta)\right), \tag{5a}$$

$$\varepsilon_r(\theta,\hat{z}) = \frac{\partial \hat{w}}{\partial r} = \frac{\hat{r}}{\hat{R}}\sum_{i=0}^{n-2} p_i(\hat{z})\varepsilon_r^i(\theta) \ , \tag{5b}$$

$$\gamma_{r\theta}(\theta,\hat{z}) = \frac{\partial \hat{u}}{\partial \hat{r}} - \frac{\hat{u}}{\hat{r}} + \frac{1}{\hat{r}}\frac{\partial \hat{w}}{\partial \theta} = \frac{\hat{R}}{\hat{r}}\left(\gamma_{r\theta}^o(\theta) + \sum_{i=1}^{n-1} f_i(\hat{z})\gamma_{r\theta}^i(\theta)\right). \tag{5c}$$

For the sake of simplicity, it is advisable to adimensionalize also the stresses with a reference stiffness. In this way, the Timoshenko beam theory considers the dimensionless circumferential force, $\hat{N}$, and the dimensionless bending moment, $\hat{M}$, by integrating the dimensionless circumferential stress, $\hat{\sigma}_\theta$, and the dimensionless shear force, $\hat{Q}$, by integrating the dimensionless shear stress, $\hat{\tau}_{r\theta}$:

$$\hat{N}(\theta) \ = \ \int_{-1}^{1} \hat{\sigma}_\theta d\hat{z} \ , \ \hat{M}(\theta) = \ \int_{-1}^{1} \hat{z}\hat{\sigma}_\theta d\hat{z} \ . \tag{6a}$$

$$\hat{Q}(\theta) \ = \ \int_{-1}^{1} \hat{\tau}_{r\theta} d\hat{z} \ . \tag{6b}$$

In the new model, new dimensionless forces and higher-order moments are required ($\hat{L}_{\theta,i}$ associated to $\hat{\sigma}_\theta$, $\hat{L}_{r\theta,i}(\theta)$ associated to $\hat{\tau}_{r\theta}$ and $\hat{L}_{r,i}$ associated to $\hat{\sigma}_r$):

$$\hat{L}_{\theta,i}(\theta) \ = \ \int_{-1}^{1} p_i(\hat{z})\hat{\sigma}_\theta d\hat{z} \ , i = 2,3,\dots,n \ . \tag{7a}$$

$$\hat{L}_{r\theta,i}(\theta) \ = \ \int_{-1}^{1} f_i(\hat{z})\hat{\tau}_{r\theta} d\hat{z} \ \ , \ \ i = 1,2,\dots,n-1 \ . \tag{7b}$$

$$\hat{L}_{r,i}(\theta) \ = \ \int_{-1}^{1} \frac{\hat{r}^2}{\hat{R}^2} p_i(\hat{z})\hat{\sigma}_r d\hat{z} \ \ , \ \ i = 0,1,\dots,n-2 \ . \tag{7c}$$

Integrating the elasticity equilibrium equations to obtain the higher-order moments equilibrium equations, integrating the constitutive law, and using the strain-displacements relations given by (5), the model final system of equations is:

$$\frac{d^2}{d\theta^2}\begin{bmatrix}\bar{L}_\theta(\theta)\\ \bar{w}(\theta)\end{bmatrix} = \bar{\bar{\omega}}_I \begin{bmatrix}\bar{L}_\theta(\theta)\\ \bar{w}(\theta)\end{bmatrix} + \bar{\omega}_N \hat{N}(\theta) \ + \bar{\omega}_M \hat{M}(\theta) \ , \tag{8a}$$

$$\bar{L}_\theta(\theta) \ = \begin{bmatrix}\hat{L}_{\theta,2} & \hat{L}_{\theta,3} & \dots & \hat{L}_{\theta,n}\end{bmatrix}^T \ \ , \ \ \bar{w}(\theta) \ = [\hat{w}_1 \quad \hat{w}_2 \quad \dots \quad \hat{w}_{n-1}]^T, \tag{8b}$$

$$\hat{N}(\theta) = \hat{N}_0 \cos\theta - \hat{Q}_0 \sin\theta \ \ , \ \ \hat{M}(\theta) = \hat{M}_0 + \hat{R}\left(\hat{N}_0 - \hat{N}(\theta)\right), \tag{8c}$$

where $\bar{\bar{\omega}}_I$ is a matrix and $\bar{\omega}_N$ and $\bar{\omega}_M$ are vectors, all of them defined from the material properties, the stacking sequence and the geometry of the beam (see [11]). $\hat{N}_0$, $\hat{Q}_0$ and $\hat{M}_0$ are the values of the respective adimensionalized force or moment at $\theta = 0$.

Regularized higher-order moments and displacements are given by:

$$\begin{bmatrix}\bar{L}_{\theta,reg}(\theta)\\ \bar{w}_{reg}(\theta)\end{bmatrix} = -\bar{\bar{\omega}}_I^{-1}\bar{\omega}_M\left(\hat{M}(\theta) + \hat{R}\hat{N}(\theta)\right) + \left(\bar{\bar{\omega}}_I + \bar{\bar{I}}_{2n-2}\right)^{-1}(\hat{R}\bar{\omega}_M - \bar{\omega}_N)\hat{N}(\theta), \tag{9}$$

where $\bar{\bar{I}}_k$ is the identity matrix of size k.

Subtracting the regularized value to the total value, perturbation higher-order moments and displacements provoked by the non-regularized magnitudes can be obtained from:

$$\frac{d^2}{d\theta^2}\begin{bmatrix}\bar{L}_{\theta,nr}(\theta)\\ \bar{w}_{nr}(\theta)\end{bmatrix} = \bar{\bar{\omega}}_I \begin{bmatrix}\bar{L}_{\theta,nr}(\theta)\\ \bar{w}_{nr}(\theta)\end{bmatrix}. \tag{10}$$

This equation can be solved analytically. The boundary conditions are given by the values of $L_{\theta,i}(0)$, $L_{\theta,i}(\Theta)$, $L_{r\theta,i}(0)$ and $L_{r\theta,i}(\Theta)$ obtained by integration through the thickness of the stresses σ_θ and $\tau_{r\theta}$ in the two ends $\theta = 0$ and $\theta = \Theta$.

Once the circumferential higher order moments, $\bar{L}_\theta$, have been obtained, circumferential stress, $\sigma_\theta(r,\theta)$, can be calculated. By using the elasticity equilibrium equations in polar coordinates the interlaminar shear stress, $\tau_{r\theta}(r,\theta)$, and the interlaminar normal stress, $\sigma_r(r,\theta)$, can be obtained.

3 COMPUTATIONAL AND CONVERGENCE CHARACTERISTICS

The main application of the method is the evaluation of the stresses in joints between two beams with distinct curvature and constant thickness. The model converges to the exact solution, but the convergence rate depends on the section selected. In sections of the beam located near to the joint the convergence is slower and presents oscillations that can be significant, requiring higher model orders to minimize these oscillations. However, the solution can be calculated with a high accuracy using lower orders, when the distance from the section to the joint increases.

As mentioned above, in a previous model, the series expansion was carried out using monomials instead of Legendre polynomials. If the same order is employed in the series expansion, the differences between the two models are associated to the errors arising from the numerical solution of the final system of equations (which are different in the two models) and the computational time needed to obtain the solution. Computational times are mainly due to the stiffness matrix calculation which is faster in the model using monomials than in the model using Legendre polynomials (since in the model using monomials all terms can be evaluated analytically, requiring much lower computational times, whereas the model using Legendre polynomials requires numerical calculation of integrals that have not yet been solved analytically).

Notwithstanding, in the model using monomials, the condition number of the matrix $\bar{\bar{\omega}}_I$ increases too fast when the order n increases. Therefore the solution of the model using monomials can only be obtained up to a certain order without inducing high errors due to the conditioning of the matrix (which depends on the minimum t/R ratio of the chains of beams).

In the model using Legendre polynomials, the condition number of the matrix $\bar{\bar{\omega}}_I$ increases much slower when the order n increases and, therefore, the solution can be obtained for any model order (obviously with a cost in the computational time).

Figure 3 shows the variation of the computational time with the order n for a single ply laminate. These times have been obtained with a computer i3 3.30 GHz and 8 GB RAM. An almost exponential variation is obtained in both models, being the computational times clearly higher in the model using Legendre polynomials. However, the model using monomials is limited by a maximum order and cannot reach a good accuracy in the vicinity of the joint.

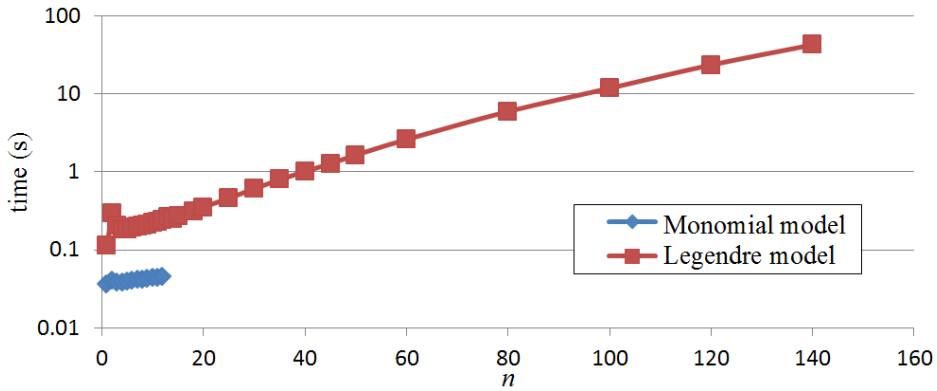

Figure 3: Computational times depending on the model order for a single ply laminate.

Computational times depend also on the number of plies of the laminate. Figure 4 shows the dependence of the computational time with the number of plies for the models using monomials and Legendre polynomials.

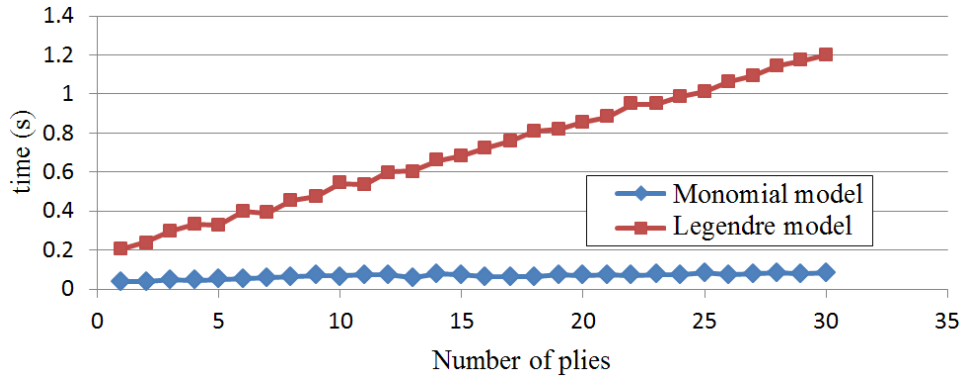

Figure 4: Computational times depending on the number of plies for $n = 10$.

The model using Legendre polynomials has higher computational times than the model using monomials due to the numerical integration mentioned before. Computational times increase linearly with the number of plies in both models, the slope being higher in the model using Legendre polynomials.

Both models are, in fact, a series expansion of the real 2D elasticity theory equations, so when the order is increased the model converges to the exact solution. Furthermore, errors are very similar for both models when the same order is chosen, but monomial model has a maximum order restriction. To exemplify the convergence of the model, Figure 5 shows the dependence of the error of the maximum radial stress in the curved part of an L-shape section (having $t = R$) with the method order. The L-shape section is composed by two semi-infinite straight beams joined to a 90º curved beam. The ply properties used are defined by E_{11}/E_{22}=20, E_{22}/G_{12}=1.7 and ν_{12}=0.3. Three different loading cases and stacking sequences have been considered, where the boundary conditions are given in the first joint, the first ply in the stacking sequence is the higher radius ply and 90º is the direction perpendicular to the 2D plane:

- Case 1: Stacking sequence: $[45,0,-45,90]_{2S}$, $\widehat{M}_0 = 1$, $\widehat{N}_0 = \widehat{Q}_0 = 0$.
- Case 2: Stacking sequence: $[45,0,-45,90]_{2S}$, $\widehat{N}_0 = 1$, $\widehat{M}_0 = \widehat{Q}_0 = 0$.
- Case 3: Stacking sequence: $[0]_{16}$, $\widehat{M}_0 = -\widehat{R}$, $\widehat{N}_0 = \widehat{Q}_0 = 1$.

By obtaining errors considering the exact solution as the one obtained by using the model using Legendre polynomials with a sufficiently high order, for several cases and for several t/R ratios, the next expression for estimating the errors is obtained:

$$\varepsilon \simeq \frac{5t}{Rn^3} \tag{11}$$

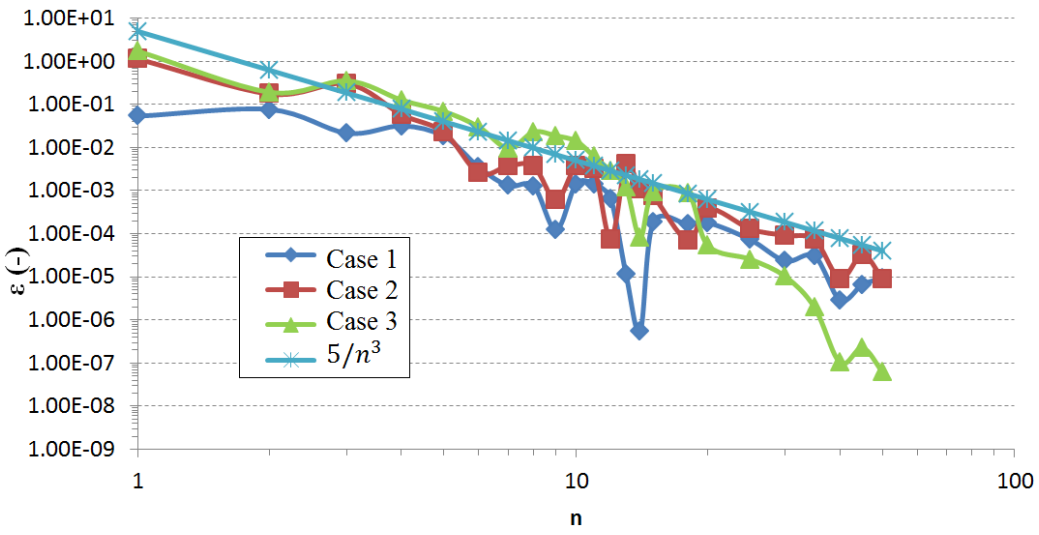

Figure 5: Error of the maximum radial stress depending on the method order for $t = R$.

Notice that model using monomials can reach only $n = 12$ if a unitary t/R ratio is chosen, coinciding with the t/R ratio that provokes an error of 1% in the maximum radial stress, which is sufficient to estimate the failure load. However, errors in the joint sections are higher and the model using Legendre polynomials is necessary to predict correctly stresses in the proximities of that section.

4 MODEL RESULTS

The model using Legendre polynomials can be applied to any geometry of continuous beams (without ramifications) of constant thickness under end loads. In this document the model is applied to three typical geometries: angles, joggles and omegas. Results show the importance of considering edge-effects in the maximum stress calculation.

4.1 Angles

Angles are typically calculated using regularized models. These kinds of models are accurate when the main force applied to the beam is the bending moment, e.g., the four point bending test. In this case, regularized stresses are the same in every section of the curved part, and the non-regularized stresses are approximately the regularized value in the middle of the curved beam. However, under other kind of loads the maximum radial and shear stresses can be localized near a joint section and the non-regularized stresses will may be significantly lower than the regularized stresses in that area. Therefore, the errors of the regularized models can reach even a 100% in these cases.

Figure 6 shows the maximum of $|\sigma_r|$ obtained at each section using the regularized solution compared with the maximum of $|\sigma_r|$ obtained at each section with the model using Legendre polynomials (with $n = 50$), in a 90º composite angle with $t = R$ (equivalent to $\hat{R} = 2$), stacking sequence $[45,0,-45,90]_{2S}$ and under axial force in one of the arms. A high difference can be observed between both distributions near to the joints, this difference being clearly reduced when moving away from the joint.

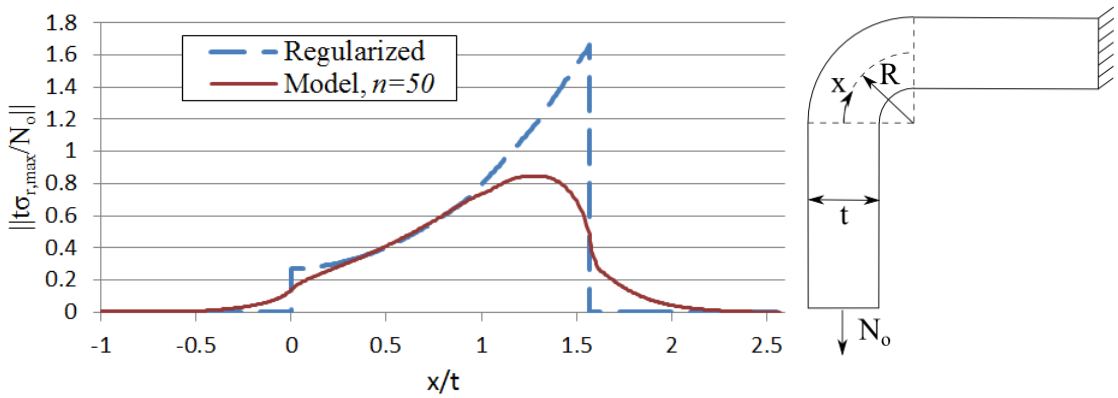

Figure 6: Comparison between regularized and real stresses in a composite angle.

It can be observed that the maximum of the regularized values of $|\sigma_r|$ is located at one of the joint sections while the maximum of the real σ_r is located in a different section. Although both sections are relatively close, it is evident that a high difference is obtained in the values of $|\sigma_r|$ obtained with the two approaches. If the failure load is determined with the regularized σ_r around a 100% difference is obtained in comparison with the failure load obtained with the model using Legendre polynomials with $n = 50$, assumable as approximately the real value. The load state shown in Figure 6 is a common loading in this kind of structural components. Therefore, a reduction in the weight of the structure may be obtained with the use of a non-regularized model, not implying an oversizing as in the regularized models.

Figure 7 shows a colour plot of the three stresses, $\sigma_\theta(r,\theta)$, $\tau_{r\theta}(r,\theta)$ and $\sigma_r(r,\theta)$, obtained with the model using Legendre polynomials with $n = 50$ for the problem defined in Figure 6.

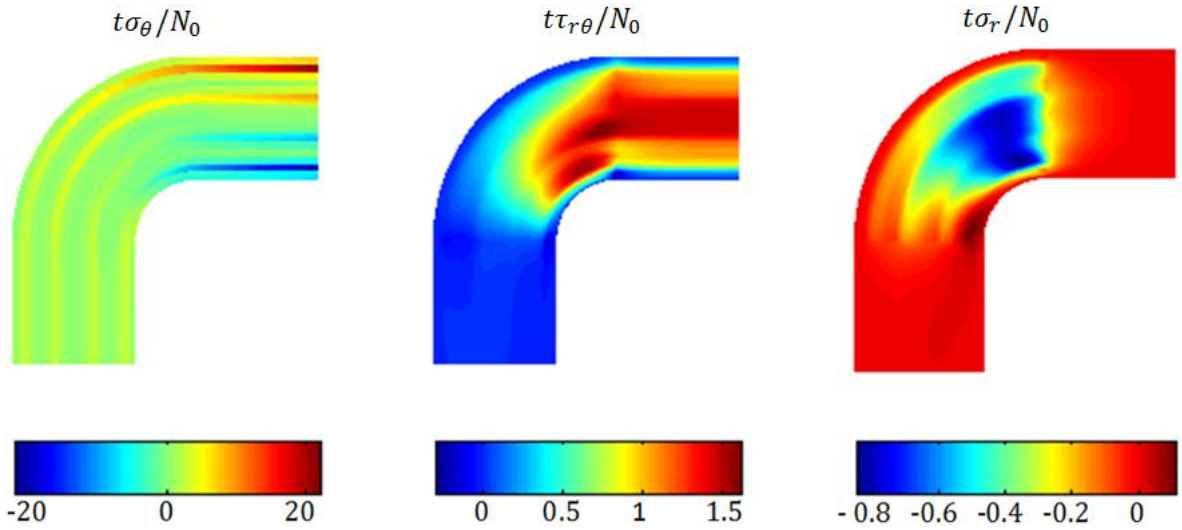

Figure 7: Stresses in a composite angle by using the model using Legendre polynomials with $n = 50$.

Notice that, while in a straight beam the distribution of the shear stresses is approximately parabolic (depending on the stacking sequence), in a curved beam the maximum of the shear stresses is situated in a smaller radius instead of the medium radius. The maximum of the radial stresses is situated nearer to the inner radius too.

4.2 Joggles

Joggles are structural elements whose section is composed by two curved parts and two long straight beams in the ends, although it can include an additional small straight part between the two curved parts. The analytic calculation of these structural elements has been usually more inaccurate when the two curved parts have small lengths $R\Theta$, since in these cases the non-regularized stresses considerably affect to the whole curved zone.

Figure 8 shows the maximum of $|\sigma_r|$ using the regularized solution compared with the maximum of $|\sigma_r|$ obtained with the model using Legendre polynomials (with $n = 50$), in the composite joggle depicted, with $t = R$ (equivalent to $\hat{R} = 2$), stacking sequence $[45,0,-45,90]_{2S}$ and under axial force in one of the arms.

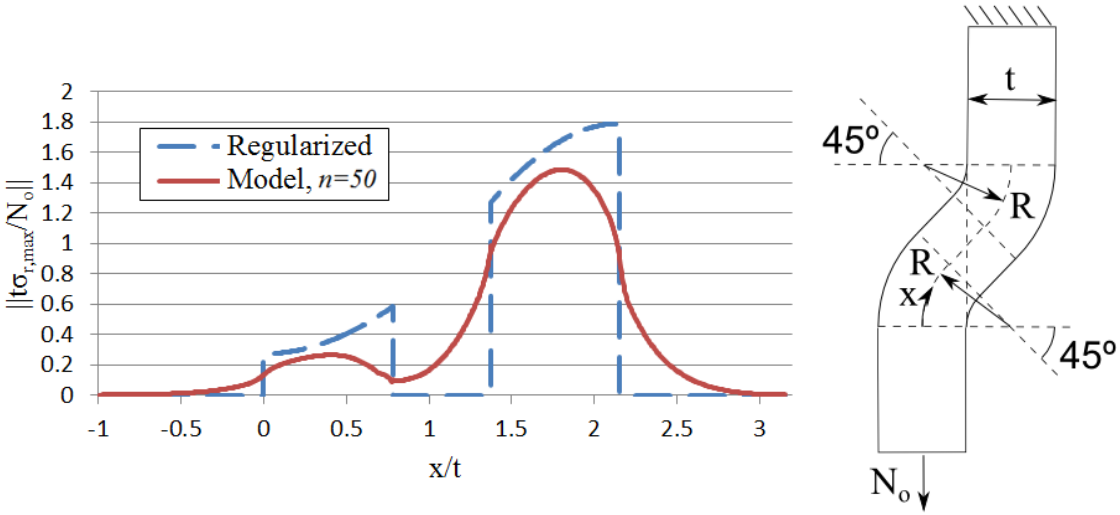

Figure 8: Comparison between regularized and real stresses in a composite joggle.

It can be observed that due to the shorter lengths of the curved zones stresses do not achieve the regularized value in any section, this case being different to the angular case. However, under this load, the maximum difference obtained in the values of $|\sigma_r|$ is lower than that obtained in the composite angle presented in the previous section.

The regularized model presents again a discontinuity in the stresses (and displacements) in the joints. Non-regularized model estimate the transition between regularized values in every pair of adjacent parts. Regularized models predict the maximum radial stress in the section of a curved beam under the maximum bending moment, the section being located in a joint. Due to the transition previously mentioned, real stresses are lower in the curved beams in the proximities of the joint, so the maximum radial stress calculated by regularized models is overestimated.

Figure 9 shows a colour plot of the three stresses, $\sigma_\theta(r,\theta)$, $\tau_{r\theta}(r,\theta)$ and $\sigma_r(r,\theta)$, obtained with the model using Legendre polynomials with $n = 50$ for the problem defined in Figure 8.

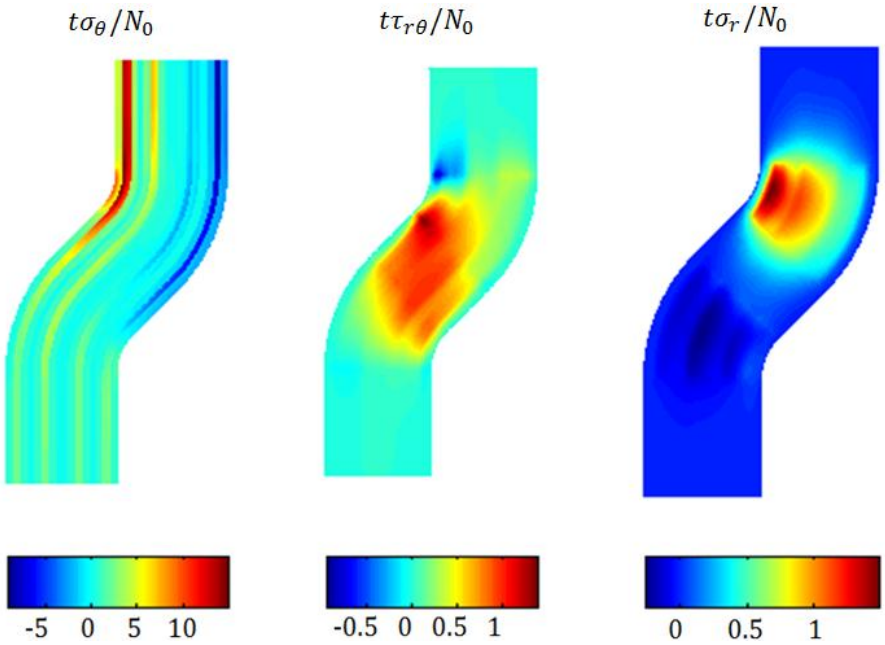

Figure 9: Stresses in a composite joggle by using the model using Legendre polynomials with $n = 50$.

Notice that, as in the L-shaped section, the maximum of the shear and the radial stresses is located nearer to the inner radius than to the outer one. Furthermore, when the inner radius is compressed in the circumferential direction the section is compressed in the radial direction, and inversely when the inner radius is tensioned in the circumferential direction the radial stresses are positive, similarly to the L-shaped section, where the first case was observed.

4.3 Omegas

Omegas are structural elements typically found in reinforcements and sandwich structures. Figure 10 shows the maximum of $|\sigma_r|$ using the regularized solution compared with the maximum of $|\sigma_r|$ obtained with the model using Legendre polynomials (with $n = 50$), in the composite omega depicted, with $t = R = L$, stacking sequence $[45,0,-45,90]_{2S}$ and under axial force in the arms.

Similarly to the joggle case, due to the shorter lengths of the curved zones stresses do not achieve the regularized value in any section. Discontinuities in the derivative of the distribution are observed in the proximities of the joint of two curved beams, where a higher curvature change is given. Those discontinuities are due to the change of the point in the section where the maximum radial stress is obtained.

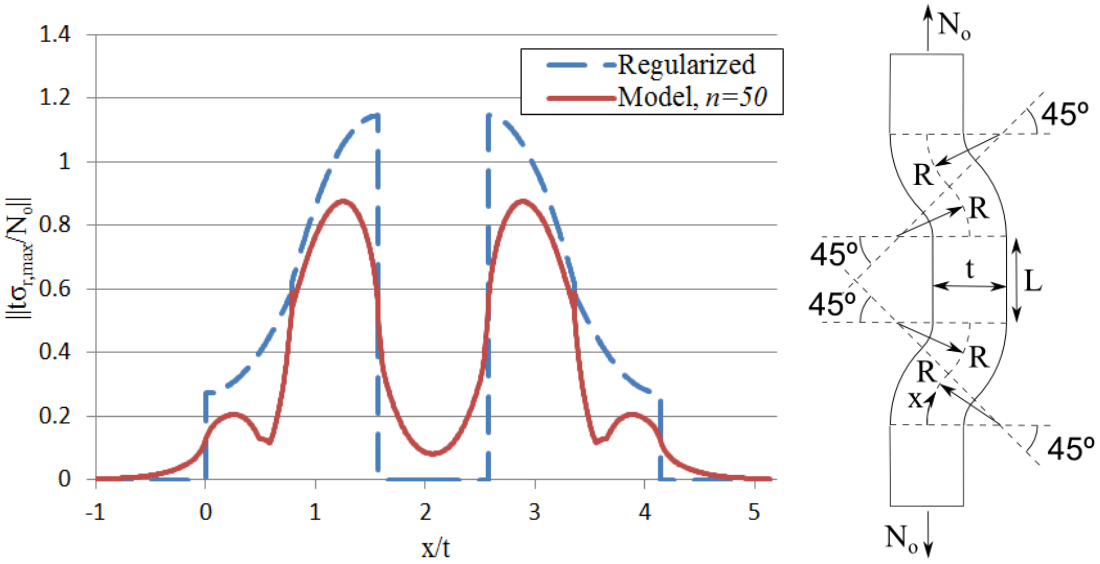

Figure 10: Comparison between regularized and real stresses in a composite omega.

Figure 11 shows a colour plot of the three stresses, $\sigma_\theta(r,\theta)$, $\tau_{r\theta}(r,\theta)$ and $\sigma_r(r,\theta)$, obtained with the model using Legendre polynomials with $n = 50$ for the problem defined in Figure 10.

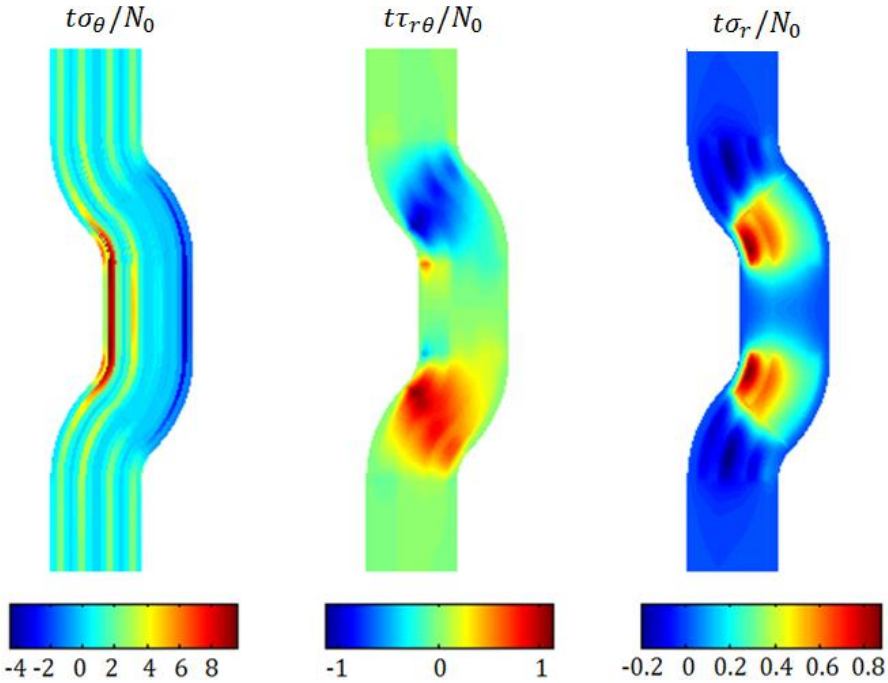

Figure 11: Stresses in a composite omega obtained with the model using Legendre polynomials with $n = 50$.

As in previous cases, sections compressed in the circumferential direction in the inner radius are compressed in the radial direction and vice versa.

If the omega is a part of the skin of a sandwich structure, an accurate calculation requires adding to the model a distributed load due to the surrounding core. This distributed load can be easily taken into account by modifying the model to include it in the equilibrium equations.

5 CONCLUSIONS

A novel method to calculate non-regularized stresses in curved composite beams based on a displacements series approximation has been developed. As has been shown, the models are applicable to many kinds of geometries, such as L-beams, C-beams, joggles, omegas, etc. The main restriction of the models, besides the 2D simplification, is that the mean line of the 2D beam should not have divisions or ramifications. Therefore, e.g., T-beams cannot be directly solved with these models. Another restriction is the constant-thickness hypothesis.

The series approximation can be either based in monomial functions or in Legendre polynomials. The model using monomials has the advantage of a high computational speed, but with the disadvantage of an order limitation due to the high increasing of the condition number of the stiffness matrix when the order increases. The model using Legendre polynomials has the advantage of an unlimited order (except for the computational limitations: time, memory, etc.) but with higher computational times. If a high accuracy is desired the model using Legendre polynomials, with a high order, is recommended.

Nowadays, design of structural elements prone to unfolding failure is carried out using either analytical models based on regularized solutions of the interlaminar stresses or using finite element models. As has been shown, regularized solutions can overestimate the maximum of the interlaminar stresses even by 100% (when the maximum interlaminar stress is located near to a joint of two laminates with different curvatures), thus oversizing structural elements. The use of finite element models requires the solution of a different model for each configuration considered. Therefore, the use of a semi-analytic model able to determine the non-regularized stresses and easy to implement in a design tool, as the one presented in this document, enables reducing the weight of the structural element in comparison with the use of analytical models based on regularized solutions or reducing the design in comparison with the use of finite elements models.

Interlaminar tensile strength in composite materials is higher than interlaminar compressive strength (that is, unfolding failure only appears when tensile interlaminar stresses are present). As has been shown, bending moments that cause tensile longitudinal stresses in the inner radius of the curved zones provoke tensile interlaminar stresses and, therefore, these bending moments will be more unfavorable than the inverse ones.

Finally, the model can be extended to consider distributed loads and variable thickness modifying the corresponding equations. The consideration of variable thickness provokes a θ dependence on the $\bar{\bar{\omega}}_I$ matrix, which may preclude the analytic resolution of equation (8a).

REFERENCES

[1] R.M. Jones. *Mechanics of Composite Materials*. Mc Graw-Hill, 1975.

[2] Martin RH. Delamination failure in a unidirectional curved composite laminate. *ASTM Special Technical Publication* (1120), pp. 365-383, 1992.

[3] S.G. Lekhnitskii, S.W. Tsai, and T. Cheron. *Anisotropic Plates*. Gordon and Breach Science Publishers, 1968.

[4] K.C. Lin and C.W. Lin. Finite deformation of 2-D laminated curved beams with variable curvatures. *International Journal of Non-Linear Mechanics*, 46(10):1293-1304, 2011.

[5] M.S. Qatu. Theories and analyses of thin and moderately thick laminated composite curved beams. *International Journal of Solids and Structures*, 30(20):2743-2756, 1993.

[6] R. Roos. *Model for Interlaminar Normal Stresses in Doubly Curved Laminates*. PhD thesis, Swiss Federal Institute of Technology, Zurich, 2008.

[7] W.L. Ko and R.H. Jackson. Multilayer theory for delamination analysis of a composite curved bar subjected to end forces and end moments. *NASA Technical Memorandum 4139*, 1989.

[8] S. Smidt. Bending of curved sandwich beams. *Composite Structures*, 33(4):211-225, 1995.

[9] J. M. González-Cantero, E. Graciani, A. Blázquez, and F. París. Evaluation of radial stresses in unfolding failure of composite materials. Analytic model. *In preparation*.

[10] J.M. González-Cantero, E. Graciani, A. Blázquez, and F. París. Analytic evaluation of radial stresses in unfolding failure of composite materials. Comparison with numerical solutions. In *Proceedings of the 16th European Conference on Composite Materials ECCM16*, 2014. 22-26 of June, Seville, Spain.

[11] J.M. González-Cantero, E. Graciani, F. París and D. Meizoso-Latova. Evaluation of non-regularized stresses in the coupling of composite beams with different curvatures with a series approximation based on Legendre polynomials. *In preparation*.

[12] H. Matsunaga. Interlaminar stress analysis of laminated composite and sandwich circular arches subjected to thermal/mechanical loading. *Composite Structures*, 60(3):345-358, 2003.

[13] S. Timoshenko. *History of strength of materials*, McGraw-Hill New York, 1953.

[14] S.P. Timoshenko. On the correction factor for shear of the differential equation for transverse vibrations of bars of uniform cross-section. *Philosophical Magazine*, p. 744, 1921.

[15] S.P. Timoshenko. On the transverse vibrations of bars of uniform cross-section. *Philosophical Magazine*, p. 125, 1922.

[16] M. Abramowitz and I.A. Stegun. *Handbook of Mathematical Functions with Formulas, Graphs, and Mathematical Tables*, Chapter 8. Dover Books on Mathematics, 1964.